

# A General Co-Simulation Approach for Coupled Field–Circuit Problems

P. Zhou, *Senior Member, IEEE*, D. Lin, W. N. Fu, B. Ionescu, *Senior Member, IEEE*, and Z. J. Cendes, *Fellow, IEEE*

**Abstract**—An indirect procedure to couple transient finite element simulation with circuit simulation is proposed. The procedure is based on extracting lumped parameters from the field simulation and Norton equivalents from the circuit simulation. This approach provides more stability and accuracy because both winding currents and terminal voltages across coupling branches are free to change. It is also more flexible since the finite element equations and the circuit equations are solved separately and allows complicated system level simulation.

**Index Terms**—Circuit simulator, field simulator, finite-element analysis, direct coupling, indirect coupling, magnetic devices.

## I. INTRODUCTION

TWO basic approaches to couple finite element analysis (FEA) with circuit simulation exist. One is the direct coupling approach [1]-[3] where the field and circuit equations are coupled directly together and solved simultaneously. The other approach is co-simulation by indirect coupling where the FEA and circuit simulator are treated as separate systems in a step-by-step process with respect to time, while they exchange coupling coefficients in each step [4], [5]. Indirect coupling becomes attractive when the time constants in the field domain and in the circuit domain differ significantly from each other. It also makes the development of individual simulators more efficient and easier to use by the experts in the different fields.

A common mechanism for indirect coupling is to use sources as coupling coefficients, where the field simulator uses the voltages across coupling windings as input and winding currents as output, while the circuit simulator uses the currents of coupling windings as input and winding voltages as output [6]. This approach provides the possibility of system level simulation. However, forcing coupling sources to be constant during a time step introduces potential convergence problems unless a very small time step is used. In addition, constant coupling current source may fail to model load commutation when a diode is directly connected to a winding. This may lead to an unphysical oscillation of the winding current or even to incorrectly keeping a diode in a permanent off state if initial winding current is zero.

In this paper, a new indirect coupling approach is presented. First, a coupling mechanism is introduced into FEA simulator to employ Norton equivalent circuits of an arbitrary external circuit system; second, the FEA simulation is enhanced to provide the circuit simulator with lumped field parameters for every coupling winding; and third, the circuit simulation is modified to feed back Norton equivalent parameters to the FEA simulator. This approach has several advantages. Not only is it more flexible in allowing FEA and the circuit simulator to work independently, the solution is more accurate and stable. This is because winding currents and voltages are both free to change across coupled windings in both the FEA simulator and the circuit simulator at each time step. In addition, the proposed approach allows the possibility of supporting system level simulation, including FEA, circuits, state machines and block diagrams.

In the following, we first explore the coupling mechanism. Then we discuss the key issue of the procedure: how to extract the lumped field coupling parameters and the Norton equivalent circuit parameters. Finally, we show three application examples.

## II. COUPLING MECHANISM

Consider FE analysis at time  $t_0$  based on the field time step  $\Delta T$ . From the field solutions, for each coupling winding, extract and send the coupling inductance matrix and induced voltages together with the winding currents to the circuit simulator. Use these coupling coefficients to perform circuit simulation from  $t_0$  to  $t_1 = t_0 + \Delta T$  in terms of a circuit time step  $\Delta t$ . This is normally much smaller than  $\Delta T$ . After performing circuit analysis from  $t_0$  to  $t_1$ , extract the Norton equivalent conductance matrix and the source currents flowing into the windings through coupling nodes from the circuit simulator. This extraction of the coupling parameters is used for the FEA embedded Norton circuit coupling at  $t_1$  and is realized by analyzing a linearized network. On the FEA side, it is more natural and more efficient to use loop current analysis. However, almost all commercial circuit simulators, such as SIMPLORER, SPICE, or Saber, use modified nodal analysis. Thus, an additional step is needed to convert the Norton equivalent circuit to Thevenin equivalent circuit form.

Since some circuit elements may experience a state change during the field time step interval  $\Delta T$  due to switching, power electronics commutation, state machine events, etc., this state

Manuscript received Jun 20, 2005.

The authors are with Ansoft Corporation, Pittsburgh, PA 15219 USA (phone: 412-261-3200; e-mail: ping@ansoft.com; dlin@ansoft.com; wfu@ansoft.com; bionescu@ansoft.com; zol@ansoft.com).

change may alter the corresponding network topology. In this case, the lumped field coupling parameters can no longer be considered as constant during the interval  $\Delta T$ , and would generate unacceptable errors. Therefore, the circuit simulator must detect the state change instant  $t'_1 = t_0 + \Delta T'$  and request the field simulator to reduce the field time step from default  $\Delta T$  to  $\Delta T'$  and then to extract the lumped field coupling parameters at  $t'_1 = t_0 + \Delta T'$ , instead of at  $t_1 = t_0 + \Delta T$ .

It is apparent from the above discussion that at a particular time point, the circuit simulator performs circuit simulation first in terms of the field coupling parameters derived at the last FEA time step. The resulting error is normally small since the winding currents are highly inductive and therefore the saturation dependent field coupling parameters will have little appreciable change during a reasonable time interval  $\Delta T$ , as long as the time step does not overstep the state change instant.

### III. COUPLING PARAMETERS

Figure 1 illustrates the co-simulation coupling parameters for a two-winding device. On the finite element side, each winding appears to the circuit simulator as a series RLE branch, with mutual inductances between the windings. On the circuit side, no matter how complicated the circuit system, the coupling nodes appear to the FEA simulator as a Norton equivalent circuit. For the mechanical subsystem, the FE simulator injects a torque into circuit simulator's mechanical model, which calculates a position that controls the finite element mesh. No parameter extraction is required for the mechanical coupling because it uses source-level coupling.

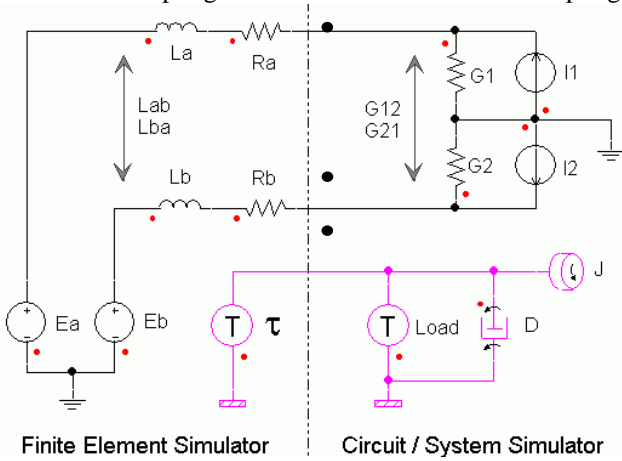


Fig. 1 Parameter coupling diagram

#### A. Field Coupling Parameter Extraction

On the finite element side, let the winding flux linkage  $\lambda$  be split into two components. One is  $Li$ , produced by coupling branch currents through the winding inductances. The other is *internal* flux linkage,  $\psi$ , produced by other sources, such as permanent magnets, other windings not connected to the coupling nodes, and induced eddy currents. Thus, the induced *terminal* voltage can be expressed as

$$\begin{aligned} e_i &= \frac{d\lambda}{dt} = \frac{d(Li)}{dt} + \frac{d\psi}{dt} \\ &= L_1 \frac{\Delta i}{\Delta t} + i_0 \frac{\Delta L}{\Delta t} + \frac{d\psi}{dt} \end{aligned} \quad (1)$$

This can also be written as

$$\begin{aligned} e_i &= L_1 \frac{di}{dt} + \frac{(L_1 i_0 + \psi_1) - (L_0 i_0 + \psi_0)}{\Delta t} \\ &= L_1 \frac{di}{dt} + \frac{\lambda'_1 - \lambda_0}{\Delta t} = L_1 \frac{di}{dt} + e_i \end{aligned} \quad (2)$$

with

$$e_i = (\lambda'_1 - \lambda_0) / \Delta t \quad (3)$$

Subscripts “1” and “0” stand for the current time point and the previous time point, respectively, and  $e_i$  is the induced *internal* voltage due to permanent magnet, motion, eddy current, the excitation of other windings not connected to coupling nodes and the contribution from  $dL/dt$ .  $\lambda'_1$  in (3) is derived under the same conditions as  $\lambda_1$ , except replacing the excitation of each coupling winding by current source with the values at previous time point. Note that the eddy effect due to the change in the winding currents has been accounted for in the equivalent inductance. The eddy effects due to other factors, such as motion, magnet, other internal sources are accounted for in the induced *internal* voltage  $e_i$ . Thus, the Thevenin equivalent of windings can be represented by an inductance  $L$  in series with an internal voltage  $e_i$ . In addition,  $R$  is used to represent either the stranded winding resistance or the solid-conductor winding resistance which is derived from the field solutions.

After FEA at each time step, the FEA system's coefficient matrix is frozen, which is equal to freezing the permeability of each element. We then solve different right-hand sides corresponding to excitation with an incremental current of 1A in each winding, one at a time, while the incremental currents in the other windings are zero. The calculated winding flux linkages provide the self and mutual inductances. The induced *internal* voltages come from the flux time derivatives as described by (3). In 3D analysis using a  $T$ - $\Omega$  formulation, the flux linkage in winding  $k$  is derived from [3]

$$\lambda_k = \iiint_{R_k} \mathbf{H}_k \cdot \mathbf{B} dR \quad (4)$$

where  $\mathbf{H}_k$  is the field corresponding to 1A current in winding  $k$  and is obtained by solving a conduction problem

$$\nabla \times \mathbf{H}_k = \mathbf{J} \quad \nabla \times \mathbf{E} = 0 \quad (5)$$

The solution domain has to be simply connected and consists of the winding and the cutting domains that fill all the holes of the winding so that a suitable boundary condition  $\mathbf{n} \times \mathbf{H}_k = 0$  can be applied without violating Ampere's law. An automatic cut domain generation algorithm was reported in [7].

#### B. Norton Circuit Coupling Parameter Extraction

On the circuit side, the Norton equivalent conductance parameters and source currents in Fig. 1 arise naturally from the modified nodal admittance algorithms used in most circuit

simulators. We can divide the nodal equation  $[G]\{v\} = \{i_s\}$  into two parts: one for internal nodes and the other for coupling nodes which connect external circuits with windings in FEA domain. Thus,

$$\begin{bmatrix} G_{cc} & G_{cn} \\ G_{nc} & G_{nn} + G_w \end{bmatrix} \begin{Bmatrix} v_c \\ v_n \end{Bmatrix} = \begin{Bmatrix} i_{sc} \\ i_{sn} + i'_{sn} \end{Bmatrix} \quad (6)$$

where  $v_c$  and  $v_n$  are internal nodal voltage vector and coupling nodal voltage vector, respectively;  $i_{sc}$  and  $i_{sn} + i'_{sn}$  are source current vector oriented towards internal nodes and coupling nodes, respectively. Here conductance sub-matrix  $G_w$  and source current  $i'_{sn}$  are the Norton equivalent representation of the windings which have become available based on the lumped coupling inductance  $L$  and internal voltage  $e_i$ . The global conductance matrix,  $G$ , corresponds to Jacobian matrix elements, and it depends on component value, and time step size. The right-hand side current source,  $i_s$ , generally represents actual sources, along with state variable history. Both sets of parameters will be non-linear, and also time-dependent in the case of switching circuits, control system interaction, and digital event simulation.

Once the circuit is linearized and solved at a FEA time point, the Norton equivalent parameters of external circuit system, including the conductance matrix  $G_e$  and the source current  $i_e$  are further extracted. This can easily be done by a following testing scheme: Let all coupling nodal voltages be zero (short-circuited); the resulting current in each coupling branch is the Norton equivalent source current. By setting one coupling nodal voltage to one and all other coupling nodal voltages to zero, the currents measured in each coupled branches is either numerically equal to self conductance (for  $v_n = 1$ ) or to mutual conductance (for  $v_n = 0$ ). Repeating this process by setting  $v_n = 1$  for each coupling node one by one gives the complete conductance matrix  $G_e$ .

#### IV. APPLICATION EXAMPLES

The first example is a four-pole, three phase spindle motor co-simulated by 3D FEA and SPICE. The stator is fed by a dc-ac inverter and the rotor is excited by permanent magnets as shown in Fig. 2. The chopped current control through controlled switches T1 – T6 maintains stator currents within the hysteresis band  $8 \pm 1A$  as shown in Fig. 3. This example demonstrates the effectiveness of the adaptive time stepping algorithm, which allows the default FE time step to be set to a very large 0.001s. However, once switching is detected, the FE time step is automatically reduced. The dots on the curves represent every computation instant with reduced minimum time step  $2 \times 10^{-5}s$ .

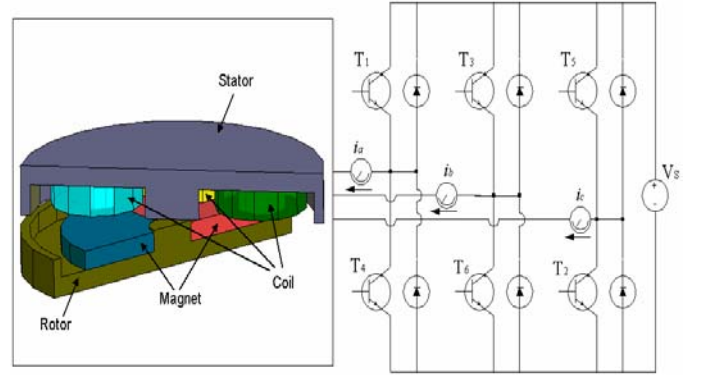


Fig. 2 Spindle motor fed by inverter with chopped-current control

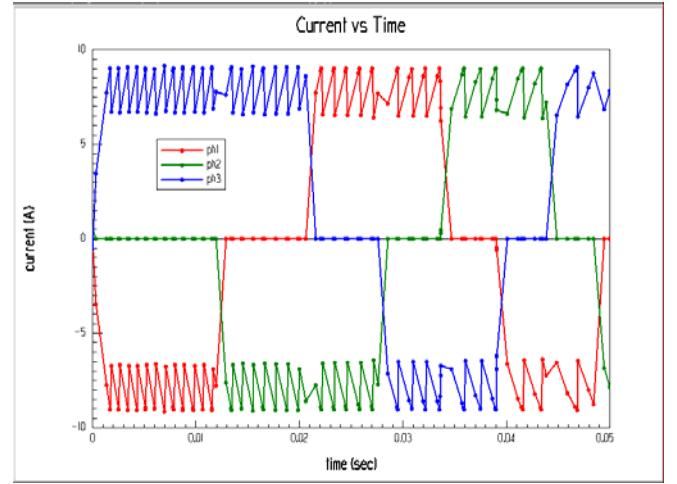


Fig. 3 Hysteresis-controlled phase currents with adaptive time step

The second example is a brushless dc motor with three phase windings shown in Fig. 4, which is co-simulated by 2D FEA with SPICE. The rating of the prototype is 900 W at 24 V; it has 11 pole pairs, 24 stator slots, and operates at 136 rpm. The permanent magnet embedded in the rotor is Nd-Fe-B and MOSFET power electronic switches used in the converter. The motor is driven by the control strategy of two-

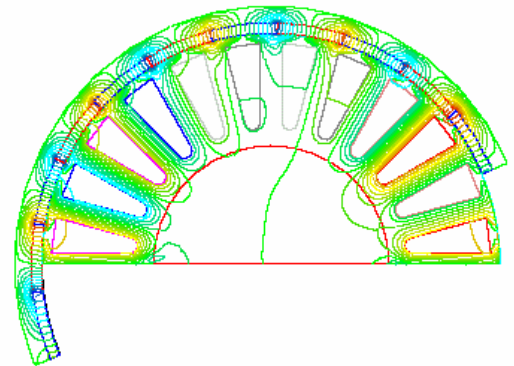


Figure 4 Flux plot of a brushless dc motor

excitation. The eddy current in the permanent magnet is taken into account by modeling the permanent magnet as a solid conductor. The computed and measured stator phase currents are shown in Fig. 5 and Fig. 6, respectively, when the motor is

fed from a PWM voltage inverter. Excellent agreement is seen between the simulated and measured results.

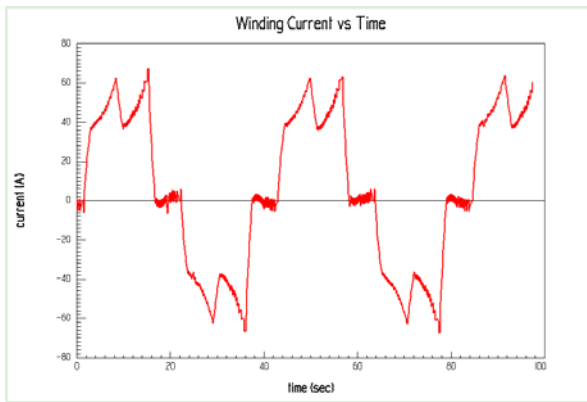


Fig. 5 Computed phase current

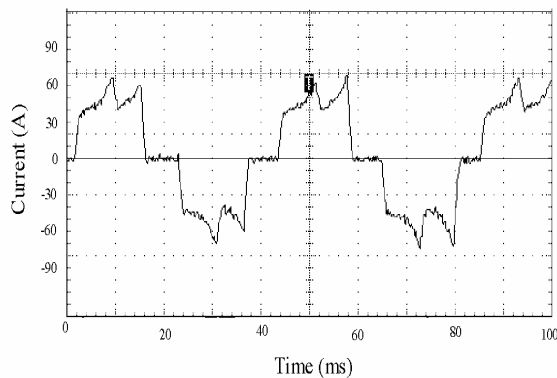


Fig. 6 Measured phase current

The third example is a 8 pole, 48-slot stator, 3 phase, 60 Hz, Y connected PM synchronous motor, which is co-simulated by 2D FEA with SIMPLORER. The stator winding has 32 turns per phase in series and is fed by the ac-dc-ac PWM inverter as shown in Fig. 7. The three-phase reference voltages are compared with a common isosceles triangular carrier wave as shown in Fig. 8. The carrier frequency of the PWM inverter is 1800 Hz. and the modulation index is 0.8. When the motor is operated at a torque angle of 15.2 electrical degrees, the computed three-phase current waveforms together with the current profile in the dc link based on the 2D FEA model are shown in Fig. 9.

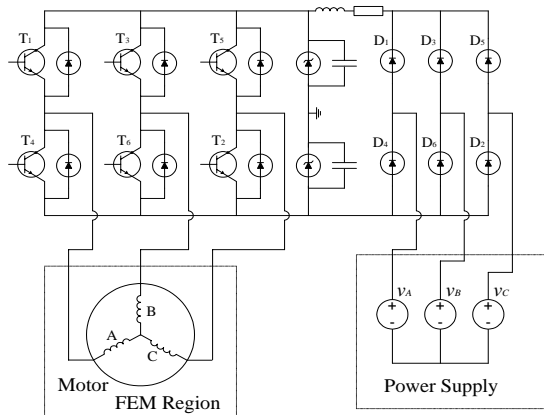


Fig. 7 PM synchronous motor fed by an ac-dc-ac inverter

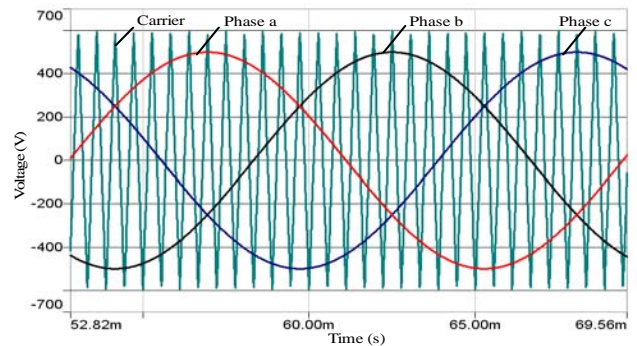


Fig. 8 Reference voltages and a common triangular carrier wave

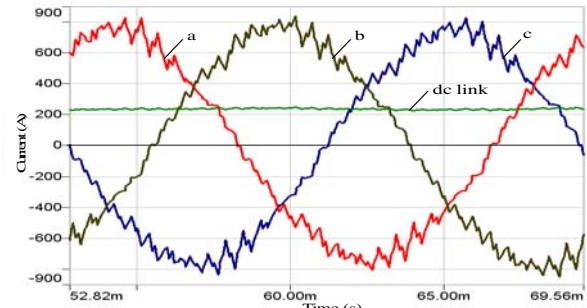


Fig. 9 Current waveforms fed by PWM

### V. CONCLUSIONS

An indirect coupling approach has been proposed based on coupling coefficient exchanges between a field simulator and a circuit simulator at each time step. The FE simulator provides the circuit simulator with lumped field parameters while the circuit simulator feeds back Norton equivalent parameters to the FE simulator. The FEA simulator has an embedded direct coupling mechanism to support the Norton equivalent representation of a circuit system. This approach is able to employ different time steps in FEA and circuit simulation and supports system level simulation with excellent stability. In addition, it makes the development of individual simulators more efficient and productive.

### REFERENCES

- [1] F. Piriou and A. Razek, "Finite element analysis in electromagnetic systems accounting for electrical circuit," *IEEE Trans. on Magnetics*, vol. 29, pp. 1669-1675, March 1993.
- [2] S. J. Salon, M. J. DeBortoli and R. Palma, "Coupling of transient fields, circuits, and motion using finite element analysis," *J. Electromagn. Waves & Appl.*, vol. 4, pp. 1077-1108, Nov, 1990.
- [3] P. Zhou, W. N. Fu, D. Lin, S. Stanton and Z. J. Cendes, "Numerical modeling of magnetic devices," *IEEE Trans. on Magnetics*, vol. 40, pp. 1803-1809, July 2004.
- [4] I. A. Tsukerman, A. Konrad, G. Meunier, and J. C. Sabonnadiere, "Coupled field-circuit problems: trends and accomplishments," *IEEE Trans. on Magnetics*, vol. 29, pp. 1701-1704, March 1993
- [5] G. Bedrosian, "A new method for coupling finite element field solutions with external circuits and kinematics," *IEEE Trans. on Magnetics*, vol. 29, pp. 1664-1668, March 1993.
- [6] S. Kanerva, "Data transfer methodology between a FEA program and a system simulator," in *Proc. IEEE-ICEMS Fifth Int. Conf.*, 2001, pp. 1121-1124.
- [7] Z. Ren, P. Zhou, and Z. J. Cendes, "Computation of current vector potential due to excitations in multiply connected conductors," in *Proc. ICEF Int. Conf.*, Tianjin, China, 2000, pp. 121-124.